Table S1. Data collection and refinement statistics

Crystal name	**Wild-type**	**Se-Met-crystal**
Space group	***R***32	***R***32
Unit cell (Å)	***a***=***b***=115.2, ***c***=157.4	***a***=***b***=114.7, ***c***=156.0
Wavelength (Å)	0.9792	0.9792
Resolution range (Å)	50-2.5 (2.59-2.50)	50-2.8 (2.91-2.80)
No. of unique reflections	14,138	11,084
Redundancy	10.7(11.1)[a]	11.0(11.2)[a]
$\boldsymbol{R}_{sym}$ (%)[b]	11.7(86.2)[a]	10.8(61.9)[a]
$\boldsymbol{I}/\boldsymbol{\sigma}$	31.3(3.7)[a]	41.1(4.6)[a]
Completeness (%)	99.8(100.0)[a]	100.0(100.0)[a]
Se sites		8
FOM		0.675
Refinement		
Resolution range (Å)	38.8~2.5	
$\boldsymbol{R}_{crystal}$ (%)[c]	23.2	
$\boldsymbol{R}_{free}$ (%)[d]	26.8	
$RMSD_{bond}$ (Å)	0.008	
$RMSD_{angle}$(°)	1.182	
Number of		
Protein atoms	1,373	
Ligand atoms	27	
Solvent atoms	5	
Residues in (%)		
most favored	93.5	
additional allowed	6.5	
Generously allowed	0	
disallowed	0	
Average B factor (Å^2) of		
Protein	45.8	
Ligand atoms	47.3	
Solvent atoms	37.3	

[a] the highest resolution shell.

[b] $R_{sym} = \sum_j \left| \langle I \rangle - I_j \right| / \sum \langle I \rangle$

[c] $\boldsymbol{R}_{\text{crystal}} = \sum_{hkl} \left| F_{obs} - F_{calc} \right| / \sum_{hkl} F_{obs}$ =

[d] $\boldsymbol{R}_{\text{free}}$, calculated the same as $\boldsymbol{R}_{\text{crystal}}$, but from a test set containing 5% of data excluded from the refinement calculation

Supplementary Figure S1

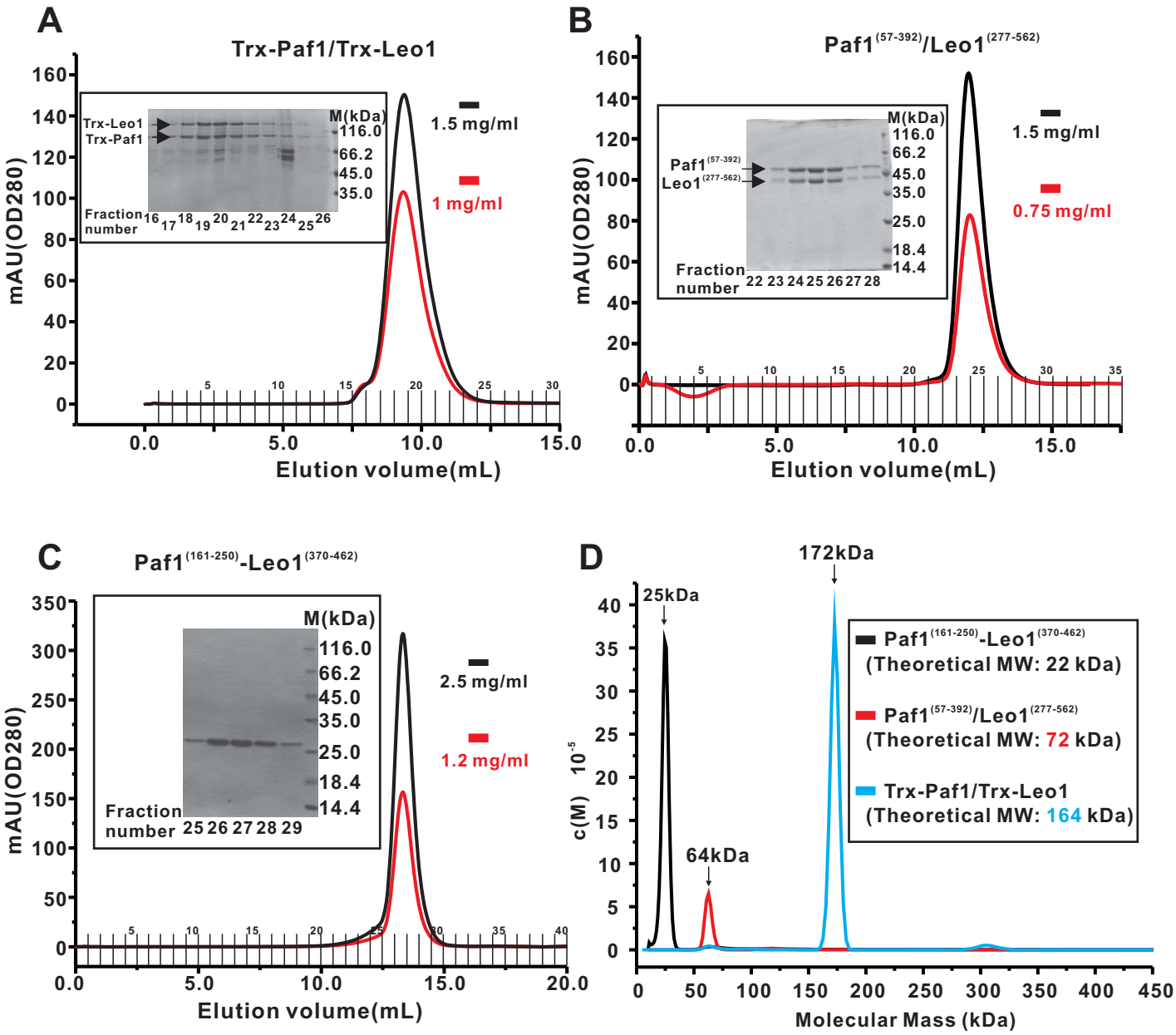

Figure S1. The Paf1/Leo1 subcomplex adopts a heterodimer with a 1:1 stoichiometry. (A, B and C) Analytical gel filtration profiles of the Trx-Paf1/Trx-Leo1 (A), the Paf1$^{(57-392)}$/Leo1$^{(277-562)}$ (B), and the single chain fusion protein Paf1$^{(161-250)}$-Leo1$^{(370-462)}$ (C) at different loading concentrations. The insets show SDS-PAGE of 15% of each fraction. (D) The molecular weights of the purified proteins were measured by analytical ultracentrifugation sedimentation velocity (SV). c(S) distributions from SV runs for the Trx-Paf1/Trx-Leo1 (1 mg/ml, cyan line), the Paf1$^{(57-392)}$/Leo1$^{(277-562)}$ (0.2 mg/ml, red line), and the Paf1$^{(161-250)}$-Leo1$^{(370-462)}$ (1 mg/ml, black line). The insert shows the theoretical MW of each protein.

Supplementary Figure S2

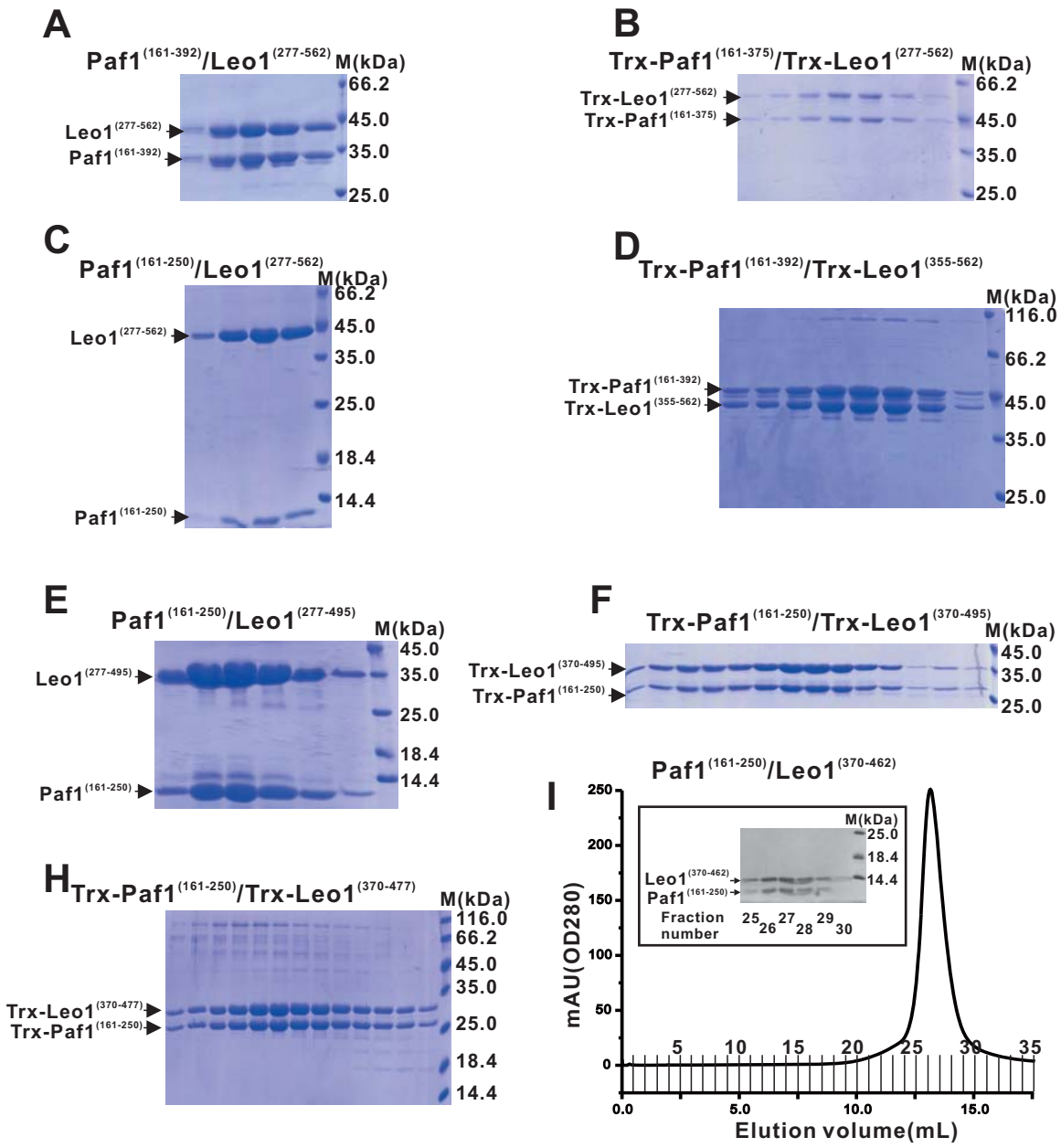

Figure S2. SDS-PAGE of various Paf1/Leo1 recombined proteins by co-expression after analytical gel filtration. For clarity, analytical gel filtration profiles are not shown, except Paf1$^{(161-250)}$/Leo1$^{(370-462)}$ complex proteins (I).

Supplementary Figure S3

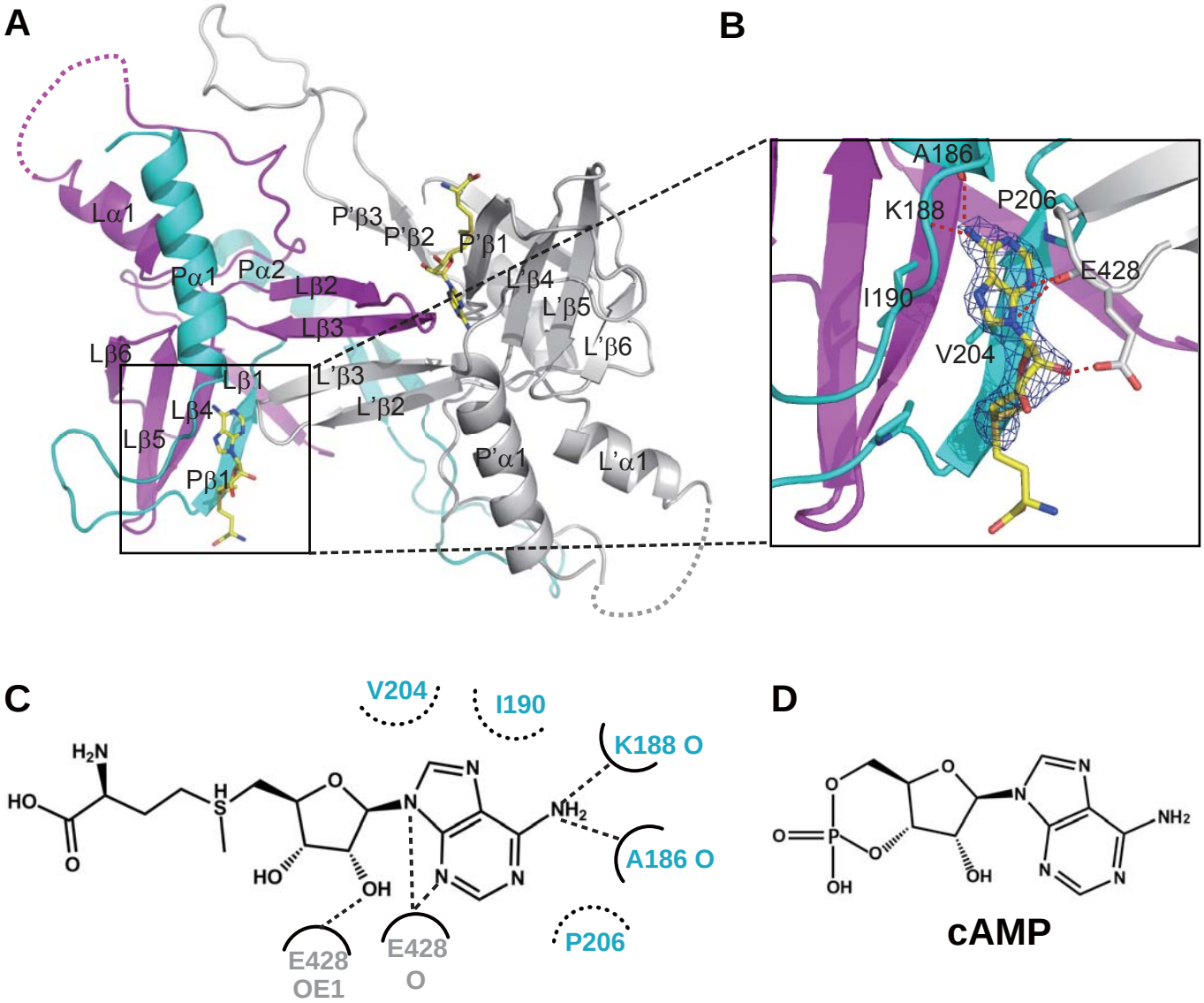

Figure S3. AdoMet in the Paf1$^{(161-250)}$-Leo1$^{(370-462)}$ heterodimer. (**A**) AdoMet may facilitate crystallization of the Paf1$^{(161-250)}$-Leo1$^{(370-462)}$ heterodimer. Only two symmetric molecules are shown for clarity. In one molecule, Paf1 and Leo1 are shown in cyan and magenta, respectively. The other symmetric molecule is shown in gray. The bound AdoMet is shown as a stick model and colored in yellow. (**B**) Omit map of AdoMet bound to the Paf1$^{(161-250)}$-Leo1$^{(370-462)}$ heterodimer. The map is contoured at the 1.5σ level and shown in blue. (**C**) The interactions formed by AdoMet with the Paf1$^{(161-250)}$-Leo1$^{(370-462)}$ heterodimer. The diagrammatic representation of the hydrogen bonds (dashed line) and hydrophobic interactions (dashed lined semicircle) formed with the AdoMet. The amino acids involved in AdoMet binding are colored in cyan and gray from Paf1 in one molecule and Leo1 in the other symmetric molecule, respectively. (**D**) Schematic structure of cAMP which could also facilitate crystal packing of the Paf1$^{(161-250)}$-Leo1$^{(370-462)}$ heterodimer.

Supplementary Figure S4

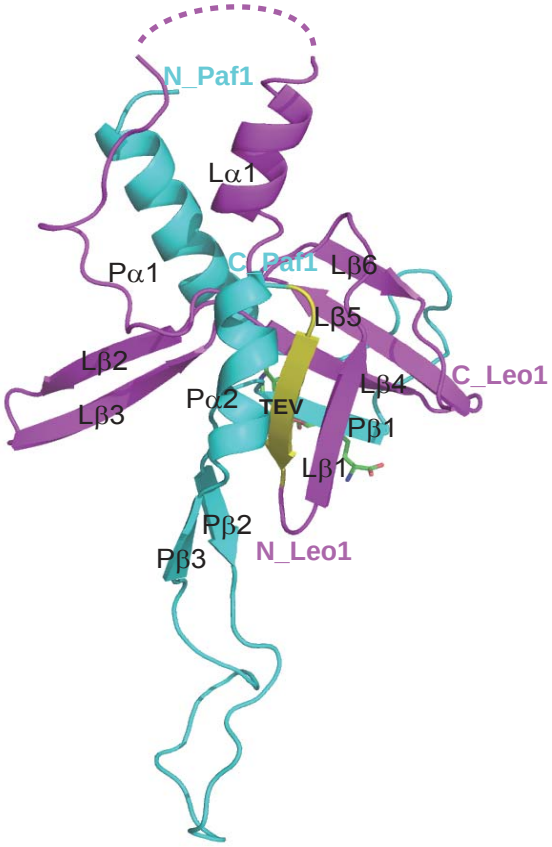

Figure S4. Cartoon representation of the overall structure of the single chain fusion of the heterodimer. Paf1$^{(161\text{-}250)}$ is shown in cyan, and Leo1$^{(370\text{-}462)}$ is shown in magenta. The β-strand formed by the TEV-cleavable linker is colored in yellow.

Supplementary Figure S5

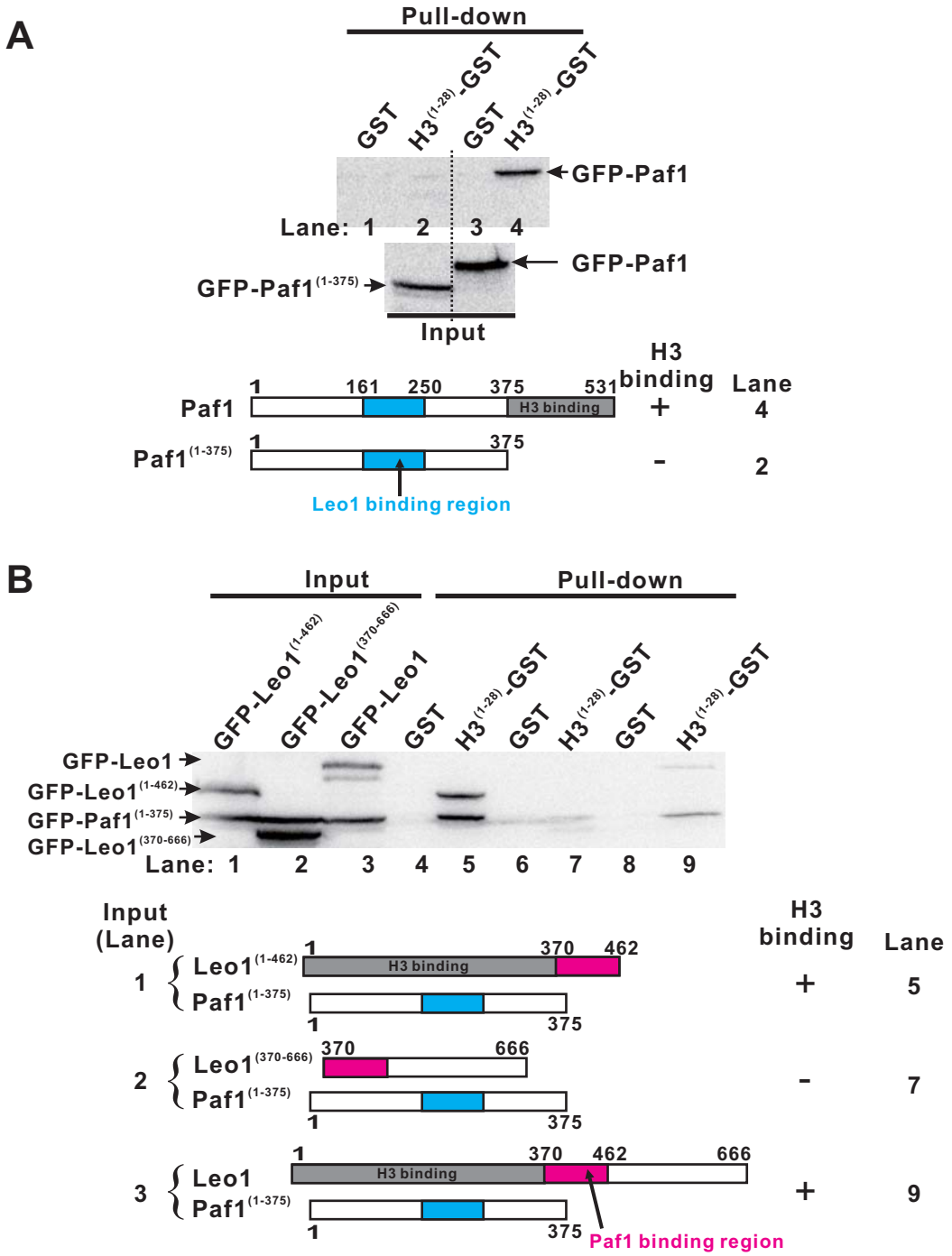

Figure S5. Histone H3 binding domain of Paf1 and Leo1. (A) and (B) The histone H3 binding domain of Paf1 and Leo1 was identified by GST pull-down assays. $H3^{(1–28)}$-GST fusion proteins were incubated with Paf1 (A, lane 4), $Paf1^{(1-375)}$ (A, lane 2), $Paf1^{(1-375)}$/$Leo1^{(1-462)}$ (B, lane 1), $Paf1^{(1-375)}$/$Leo1^{(370-666)}$ (B, lane 2), and $Paf1^{(1-375)}$/Leo1 (B, lane 3), respectively. The PVDF membrane was immunoblotted with α-GFP. The Input lanes of (A and B) represent 20% of the input material for the corresponding pull-down. The cartoon shows the results obtained in the GST pull-down assays. "+" or "-" indicates binding or no binding, respectively, between $H3^{(1-28)}$-GST and the corresponding protein or protein complexes. The schematic representation of the full length and mutant constructs used in the GST pull-down assays.

Supplementary Figure S6

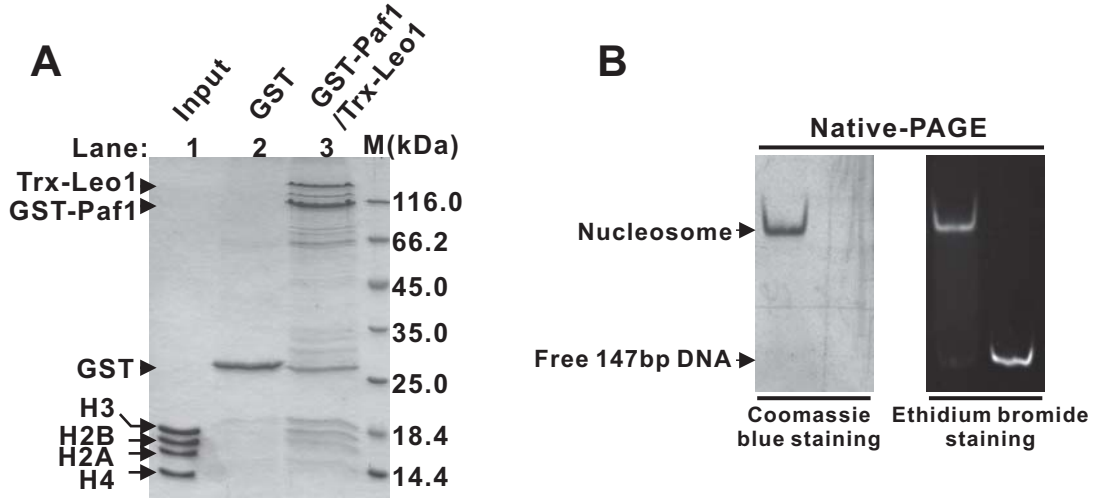

Figure S6. The Paf1/Leo1 subcomplex interacts with the recombined histone octamer. (A) GST pull-down assays of the Paf1/Leo1 subcomplex with histone octamer. GST-Paf1/Trx-Leo1 complex fusion proteins (lane 3) or GST alone (lane 2) were incubated with reconstituted histone octamer. Lane 1 shows 50% of the input for the pull-down. The SDS-PAGE gel was stained with Coomassie Blue. (B) Native-PAGE of nucleosome. Recombinant histone octamer assembled with a 147bp DNA sequence. The native-PAGE gel was stained with Ethidium bromide (right panel), and then stained with Coomassie Blue (left panel).

Supplementary Figure S7

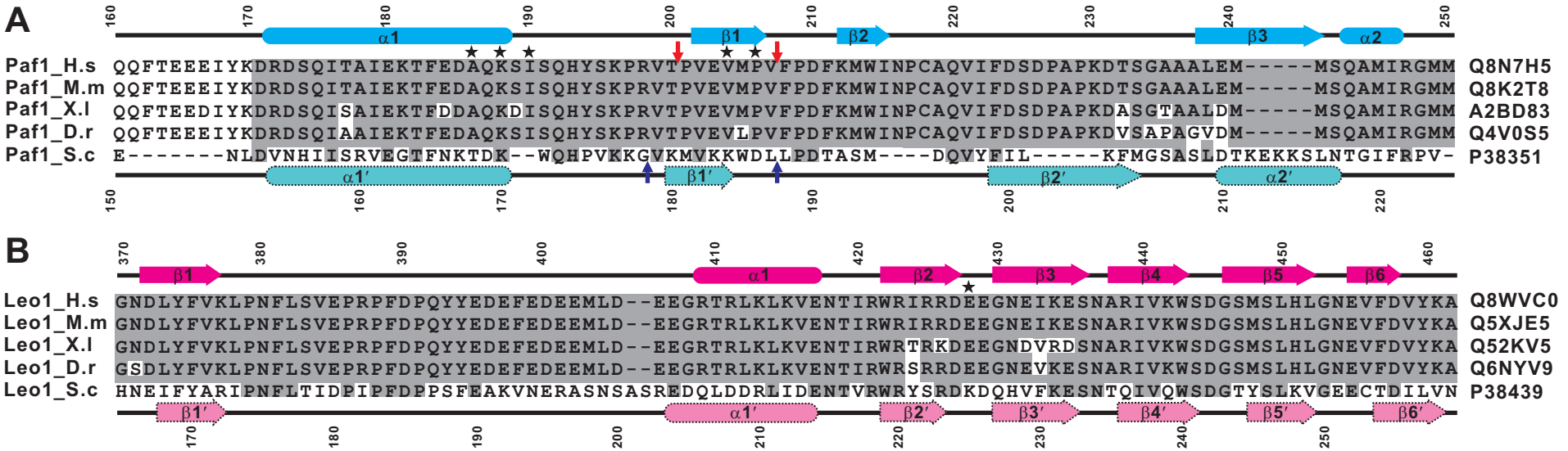

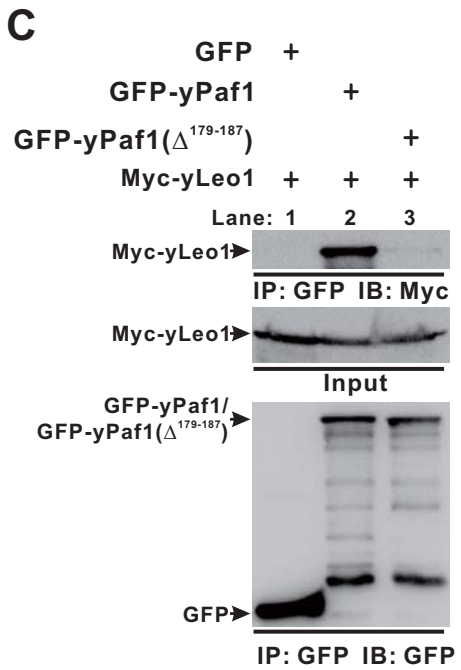

Figure S7. Paf1/Leo1 subcomplex forms a heteromeric complex through the similar mechanism between yeast and metazoan species. (**A**) and (**B**) Structure-based sequence alignment of Paf1 and Leo1 from different species**.** In this alignment, the secondary structures of H.s Paf1$^{(161\text{-}250)}$ (A) and Leo1$^{(370\text{-}462)}$ (B) are shown at the top, the predicted secondary structures of S.c Paf1$^{(150\text{-}225)}$ (A) and Leo1$^{(165\text{-}259)}$ (B) (analyzed by the NPS@ Web server) are shown at the bottom of each sequence. The identified residues of Paf1 and Leo1 are shaded with grey. The amino acids involved in the interaction between the Paf1$^{(161\text{-}250)}$/Leo1$^{(370\text{-}462)}$ heterodimer and AdoMet are marked by stars. The amino acids of Pβ1, which was deleted in Paf1(ΔPβ1) construct, are marked between the red arrows. The amino acids 179-187 of yeast Paf1, which was deleted in GFP-yPaf1(Δ$^{179\text{-}187}$) construct, are marked between the blue arrows. The GenBank numbers are shown at the end of each alignment. Species abbreviations: H.s, Homo sapiens; M.m, Mus musculus; X.l, Xenopus laevis; D.r, Danio rerio; S.c, Saccharomyces cerevisiae. (**C**) Co-IP experiment of the interaction between yeast Leo1 (yLeo1) with wild-type and mutant yeast Paf1 (yPaf1). The top panel shows the immunoprecipitation (IP) results. The middle panel represents 20% of the input material Myc-yLeo1 for each IP. The bottom panel represents the IP of GFP, GFP-yPaf1, and GFP-yPaf1(Δ$^{179\text{-}187}$).

Supplementary Figure S8

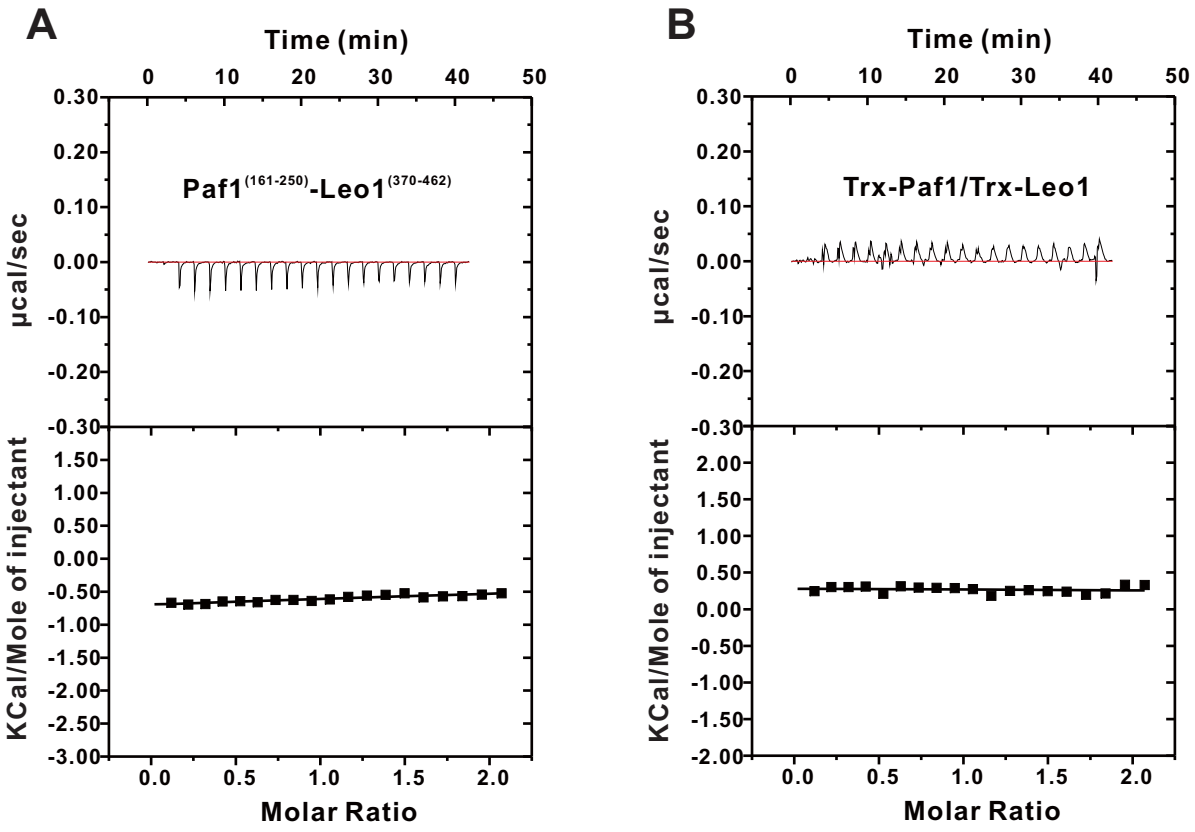

Figure S8. Interaction of the Paf1/Leo1 subcomplex with the AdoMet was tested by isothermal titration calorimetry (ITC). 500 and 1800 µM AdoMet were titrated into the calorimeter cell filled with the purified Paf1$^{(161-250)}$-Leo1$^{(370-462)}$ protein solution (50 µM) (A) and the Trx-Paf1/Trx-Leo1 (180 µM) (B), respectively. ITC results indicated no interaction between Paf1/Leo1 subcomplex and AdoMet.